Chapter 6

Parkfield-Hollister electromagnetic monitoring array

Sierra Boyd & H. Frank Morrison
Dept. of Materials Science and Mineral Engineering
University of California, Berkeley.

1. Introduction

In 1995 UC Berkeley installed magnetotelluric (MT) observatories at two locations along the San Andreas Fault to monitor possible changes in the electromagnetic (EM) fields associated with earthquakes (Fraser-Smith, 1994). Since then MT data have been continuously recorded at 40 Hz and 1 Hz and archived at the NCEDC. During this past year EM data during the largest and closest earthquake to date were recorded. On August 12, 1998 the MT array consisting of two sites, Parkfield (PKD1) and Hollister (SAO), measured the electric and magnetic fields during a M_w 5.1 earthquake in San Juan Bautista. These data are of particular interest due to the earthquake's large magnitude and close proximity to the Hollister site, SAO. EM and seismic time series will be presented below.

This last year has also seen the relocation of the temporary Parkfield site from Haliburton Ranch, PKD1, to a permanent site at Bear Valley Ranch, PKD. In early February 1999, a permanent MT observatory was installed 12 km from the temporary Parkfield site, PKD1. For just under a month, the array of three MT observatories simultaneously recorded data until the temporary site was removed.

2. Magnetotelluric array

The MT observatories are located at Parkfield (PKD1, PKD) 300 km south of the San Francisco Bay Area and Hollister (SAO), halfway between San Francisco and Parkfield. Sites PKD1 and SAO, separated by a distance of 150 km, are each equipped with three induction coils and two 100 m electric dipoles. The permanent Parkfield site (PKD) is similarly equipped with an additional pair of 200 m electric dipoles for noise cancellation purposes. All data are fed to Quanterra dataloggers, shared with collocated BDSN stations, synchronized in time by GPS and sent to NCEDC via telephone lines. During the overlap period when all three sites were operational, the seven additional channels of data from the new site enabled us to measure a decrease in the residual noise power spectrum at PKD1 as seen in Figure 6.1. The residual power is basically the threshold for detecting anomalous signals that might be generated by a local source. As intended the array is providing sensitivity to such anomalous fields at roughly 30 times the sensitivity of field detection at a single station. The black curve at the top is the total power spectrum of the west component of the horizontal magnetic field, Hx, at the temporary site in Parkfield, PKD1. The other curves are the residual power spectra derived from pairs of channels, either electric or magnetic, from all three sites. The minimum residual power spectrum shown in green is the difference between Hx at PKD1 and the predicted Hx using the horizontal magnetic fields from PKD, 12 km away. This demonstrates the advantage of having at least two sites in close proximity of one another to increase the sensitivity of detecting anomalous signals.

3. Preliminary results: M_w 5.1 earthquake, San Juan Bautista, CA, August 12 1998

A M_w 5.1 earthquake occurred at 14:10:25.11 UTC (36.7533 -121.4618) August 12 1998 on the San Andreas Fault 12 km SSE of San Juan Bautista at a depth of

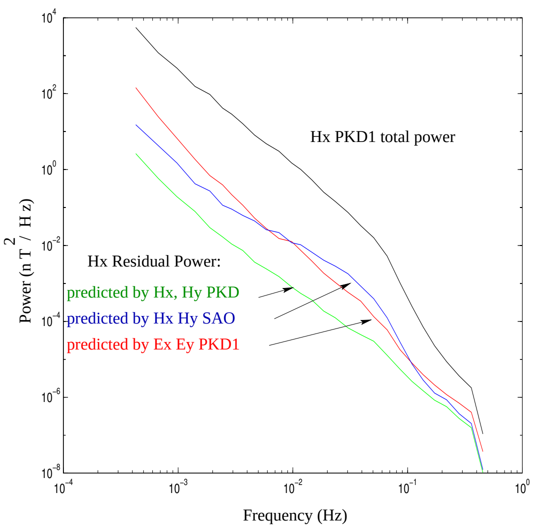

Figure 6.1: Hx total and residual power spectra at PKD1 averaged over 8 days. *Courtesy of S. Boyd.*

9.2 km. There were several foreshocks including a M_L 3.14 event at 14:02:47.21 UTC (36.7517 -121.4557, depth 8.6 km), 7.6 minutes before and a M_L 2.80 event at 12:54:04.59 UTC (36.7525 -121.4580, depth 8.11 km) 1.3 hours before the mainshock (Uhrhammer et al., 1999). During these earthquakes all five EM sensors were functioning at Hollister. However, only three of five data channels from Parkfield were useable as a result of equipment failure.

3.1 Visual inspection in the time domain

A visual inspection of the 40 Hz Hollister EM time series reveals some interesting features due to both cultural and natural sources. One such feature includes a 3.5 to 8 Hz sinusoidal signal on the horizontal electric field channels starting the third week in July 1998 and ending sometime during the last week in August 1998. The signal occurs approximately every 20 minutes and is about 4 minutes in duration, suggesting a man-made source. The sinusoidal signal is preceded by a spike of 40 mV and appears stronger on the north dipole. The frequency of the signal gradually increases and then abruptly ends. There is no corresponding signal on the magnetic field data.

The EM sensors are also sensitive to ground motion. As the surface seismic waves propagate, the energy displaces both the electrode dipole cables and the induction coils, creating signals. For example, when the electrode line is moved by wind or ground motion, a signal is generated by the motion of the wire in a magnetic field. Similarly, when the coil tilts as a result of ground motion, the magnetic flux through the coil varies creating an induced signal.

Ten seconds of raw EM and seismic time series from Hollister and Parkfield are presented in Figure 6.2. There is a correlated signal associated with the mainshock and subsequent ground shaking at Hollister seen in the Hollister EM and seismic time series, left plot Figure 6.2. The upper five traces are EM data starting with the horizontal electric fields followed by three components of the magnetic field. The fifth trace is the vertical component of the magnetic field which suffers the largest excursion most likely as a result of the sensor tilting in the hole. Below the EM data are low and high sampled seismic data. On the right plot are EM data from PKD1 shown in the top five traces and seismic data from both PKD1 and PKD, shown below. There is an anomalous spike on the magnetic field channels at Parkfield over 100 miles away from the earthquake as shown on the right side of Figure 6.2, in particular the vertical component, fifth trace. Could this be an electromagnetic signal generated coseismically at Hollister and propagated in the air to PKD1? The mechanism for such an EM field is presently unknown. This is followed by a delayed chirp-like pulse on the three accelerometers located 100 m away from the PKD1 coils shown on the same plot of Figure 6.2, traces 6-8. One explanation for these signals could be local ground motion at PKD1 since there is no corresponding signal on seismic traces 9 and 10 from PKD which is 12 km away. Approximately 20 seconds after the mainshock at Hollister, the seismometers and accelerometers at PKD recorded ground motion, from the Hollister event, followed by the EM sensors and accelerometers at PKD1 (data not shown here).

The analysis of intersite transfer functions revealed the influence of the Bay Area Rapid Transit (BART) system as far away as Parkfield and also indicated that BART may actually influence the generation of fields in the magnetosphere (Egbert et al., 1999). The extraction of such information from the array data is another indication of the high sensitivity to anomalous EM fields.

4. Acknowledgments

This work was done in collaboration with G.D. Egbert, College of Oceanic and Atmospheric Sciences, Oregon State University, Corvallis, OR.

This work was funded by USGS grant number 1434-HQ-97-GR-03076.

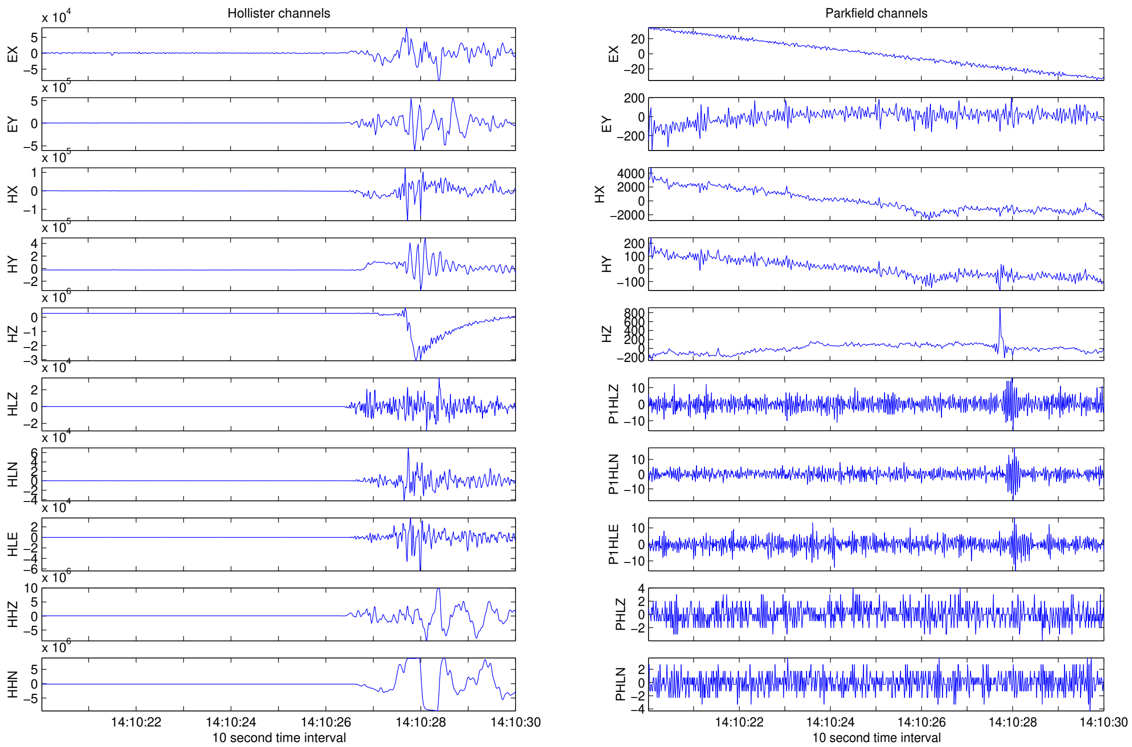

Figure 6.2: Ten seconds of raw EM and seismic time series: Hollister data on the left and Parkfield data on the right. Vertical scale is counts and horizontal scale is time. Top five traces are EM data: 2 electric field channels, 2 horizontal magnetic field channels and the vertical magnetic field. The lower five traces are seismic data. Traces 6-8 are 1 Hz sampled seismic data; traces 9 and 10 are 80 Hz sampled seismic data. From Parkfield the 1 Hz seismic data comes from both PKD1, traces 6-8, and PKD, traces 9 and 10. Note, the first EM channel from Parkfield, Ex, is down. *Courtesy of S. Boyd.*

5. References

Egbert, G.D., M. Eisel, O.S. Boyd and H.F. Morrison, DC trains and Pc3s: Source effects in mid-latitude geomagnetic transfer functions, *Geophys. Res. Lett.,* accepted 1999.

Egbert, G.D., Robust Multiple-Station Magnetotelluric Data Processing, *Geoph. J. Int., 130,* 475-496, 1997.

Fraser-Smith, A.C., A. Bernardi, P.R. McGill, M.E. Ladd, R.A. Helliwell and O.G. Villard, Jr., Low Frequency Magnetic Field Measurements near the Epicenter of the Ms 7.1 Loma Prieta Earthquake, *Geophys. Res. Lett., 17,* 1465-1468, 1990.

Uhrhammer, R., L. Gee, M. Murray, D. Dreger, and B. Romanowicz, The M_w 5.1 San Juan Bautista, California Earthquake of 12 August 1998, *Seism. Res. Lett.,70,* 10-18, 1999.

Chapter 7

Data Archive and Distribution: Northern California Earthquake Data Center

Douglas Neuhauser, Stephane Zuzlewski, Rick McKenzie, Steve Fulton, Lind Gee

1. Overview

The Northern California Earthquake Data Center, a joint project of the Berkeley Seismological Laboratory and the U.S. Geological Survey at Menlo Park, serves as an "on-line" archive for various types of digital data relating to earthquakes in central and northern California. The NCEDC is located at the Berkeley Seismological Laboratory, and has been accessible to users via the Internet since mid-1992.

The primary goal of the NCEDC is to provide a stable and permanent archival and distribution center of digital geophysical data for northern and central California such as seismic waveforms, electromagnetic data, GPS data, and earthquake parametric data. The principal networks contributing seismic data to the data center are the Berkeley Digital Seismic Network (BDSN) operated by the Seismological Laboratory, the Northern California Seismic Network (NCSN) operated by the USGS, and the Bay Area Regional Deformation (BARD) GPS network. The collection of NCSN digital waveforms date from 1984 to the present, the BDSN digital waveforms date from 1987 to the present, and the BARD GPS data date from 1993 to the present.

The NCEDC continues to use the World Wide Web as a principal interface for users to request, search, and receive data from the NCEDC. The NCEDC has implemented a number of useful and original mechanisms of data search and retrieval using the World Wide Web, which are available to anyone on the Internet. All of the documentation about the NCEDC, including the research users' guide, is available via the Web. Users can perform catalog searches and retrieve hypocentral information and phase readings from the various earthquake catalogs at the NCEDC via easy-to-use forms on the Web. In addition, users can peruse the index of available broadband data at the NCEDC, and can request and retrieve broadband data in standard SEED format via the Web. Access to all datasets is available via research accounts at the NCEDC. The NCEDC's home page address is `http://quake.geo.berkeley.edu/`

2. Datasets

The initial phase of archiving the historic NCSN earthquake seismograms from 1984 through the present and BDSN data from 1987 through the present is basically complete. All historic NCSN data tapes have been read and data for all local and regional events have been loaded onto the NCEDC. A list of teleseismic events recorded by the NCSN is now available on the NCEDC, and the NCSN is determining which of those event have sufficient data to archive at the NCEDC. The 16-bit BDSN data from 1987-1991 have been converted to MiniSEED and are now online.

The total size of the datasets archived at the NCEDC is shown in Table 7.1.

2.1 BDSN/HFN Seismic Data

The archival of current BDSN and HFN seismic data is an ongoing task. BDSN and HFN data are telemetered from 29 seismic dataloggers in real-time to the BSL, where they are written to disk files. Each day, an extraction process creates a daily archive by retrieving all continuous and event-triggered data for the previous day. The daily archive is run through quality control procedures to correct any timing errors, triggered data is

Data Type	MBytes
Broadband, electric field , and magnetic field waveforms (compressed)	484,411
NCSN event seismograms (compressed)	197,717
GPS data (compressed RINEX and raw data)	122,863
Unocal Geysers region seismograms	25,090
Parkfield HRSN seismograms	2,728
Misc data	8,920
Total size of archived data	841,729

Table 7.1: Volume of Data Archived at the NCEDC by Data Type

reselected based on the REDI, NCSN, and UCB earthquake catalogs, and the resulting daily collection of data is archived at the NCEDC.

2.2 NCSN Seismic Data

NCSN waveform data continue to be collected and processed by the USGS at Menlo Park, and shipped to the datacenter on exabyte tapes. The NCSN has developed procedures to send event waveform files from Menlo Park to the NCEDC via the Internet, but was delayed by TCP/IP software problems on the Vax computers at Menlo Park. New software has been acquired that fixes the problem, and we should be able to initiate that process shortly. Parametric information, such as event catalogs and phase readings from both the BDSN and NCSN networks are automatically updated on the NCEDC on a daily basis.

Various problems were encountered that prevented the NCEDC from loading many of the NCSN waveforms. First, it was discovered that a significant number of waveforms were erroneously loaded by the NCEDC in VAX (little-endian) byteorder instead of the Sun (big-endian) byteorder used at the NCEDC. In addition, problems with the hardware on the new mass storage system and software for the old mass storage system significantly delayed the migration of data from the old mass storage system to the new mass storage system. Since no additional space was available on the old mass store, we needed to migrate the old data to the new mass store before fixing the byte ordering problem with the existing datafiles. In addition, we needed to fix the byte ordering problem before loading new NCEDC data onto the mass store. As a result, we have a significant backlog of current NCSN data to archive at the NCEDC.

2.3 Electro-Magnetic Data

The NCEDC continues to archive and process electric and magnetic field data acquired from 3 dataloggers at three sites (SAO, PKD, and PKD1). At PKD and SAO, 3 components of magnetic field and 2 or 4 components of electric field are digitized and telemetered in real-time along with seismic data to the Seismological Laboratory, where they are processed and archived at the NCEDC in a similar fashion to the seismic data. The system generates continuous data channels at 40 Hz, 1 Hz, and .1 Hz for each component of data. All of these data are archived and remain available online at the NCEDC. Using programs written by Dr. Martin Fullerkrug at the Stanford University STAR Laboratory, the NCEDC is computing and archiving magnetic activity and Schumann resonance analysis using the 40 Hz data from this dataset.

The datalogger at PKD1 acquires 8 channel of low frequency long baseline electric field data from an ongoing project by Dr. Steve Park of UC Riverside. This data is acquired and archived in an identical manner to the other electric field data at the NCEDC.

2.4 GPS Data

The NCEDC continues to expand its archive of GPS data through the BARD (Bay Area Regional Deformation) network of continuously monitored GPS receivers in northern California. The NCEDC GPS archive now includes 40 sites in northern California. There are 25 core BARD sites owned and operated by UC Berkeley, LLNL, USGS, UC Davis, Trimble Navigation, and Stanford. Data from the other northern California sites are collected from sites operated by JPL, the US Coast Guard, and Scripps Institute of Oceanography.

Most of the Berkeley BARD sites are co-located with seismic stations, and data from these sites are acquired in real-time using shared frame relay telemetry link. The remaining Berkeley BARD stations use dedicated frame relay and/or spread spectrum radio to provide data in real-time to UC Berkeley, and are automatically processed and archived at the NCEDC on a daily basis. Data from the USGS sites are downloaded by the USGS and transferred to the NCEDC on a daily basis, and is automatically archived by the NCEDC. The other sites are automatically acquired from their respective operators on an hourly or daily basis, and are archived by the NCEDC.

The NCEDC is participating in the UNAVCO-sponsored GPS Seamless Archive Centers (GSAC) initiative, which is developing common protocols and interfaces for the exchange and distribution of continuous and survey-mode GPS data.

2.5 Unocal Seismic Data

The Unocal Corporation operated a micro-seismic monitoring network in the Geysers regions of northern California. In prior years, Unocal had released six years of triggered event waveform data from 1987-1994 for archival and distribution at the NCEDC. Through an updated agreement with the NCEDC this year, Unocal released triggered event waveform data and a preliminary hypocenter catalog for an additional four years of data from 1995-1998. The total dataset represents over 150,000 events that were recorded by the Unocal Geysers network, and is available via research accounts at the NCEDC. Although Unocal did not release a preliminary hypocenter catalog for the first six years of data or phase readings for any of the events, several scientists have already deemed this dataset as a useful addition to the NCEDC. Due to problems encountered with the tape media used by Unocal to archive their data, the NCEDC is still loading portions of the 1995-1998 data.

2.6 Parkfield High Resolution Seismic Network Data

Event seismograms from the Parkfield High Resolution Seismic Network from 1987 through June 1998 have been loaded onto the NCEDC in their raw SEGY format. A number of events have faulty timing due to the lack or failure of a precision timesource for the network. Due to funding limitations, there is currently no ongoing work to correct the timing problems in the older events or to create MiniSEED volumes for these events. However, a preliminary catalog for a significant number of these events has been constructed, and the catalog is available via the web at the NCEDC. The raw SEGY data files are available via research accounts at the NCEDC.

2.7 CNSS Worldwide Earthquake Catalog

The NCEDC, in conjunction with the Council of the National Seismic System (CNSS), is producing and distributing a world-wide composite catalog of earthquakes based on the catalogs of the national and various US regional networks. Each network updates their earthquake catalog on a daily basis at the NCEDC, and the NCEDC constructs a composite world-wide earthquake catalog by combining the data, removing duplicate entries that may ocurr from multiple networks recording an event, and giving priority to the data from each network's *authoritative region*. The catalog, which includes data from 14 regional and national networks, and is available for use at the NCEDC, and is made available to anyone over the Internet.

3. New Facilities and Hardware

The NCEDC moved into new facilities at the newly renovated Berkeley Seismological Laboratory in McCone Hall in January 1999. This move reunited all of the NCEDC mass storage systems and computers into a single location and onto the same high-speed 100 MBit switched network.

Last year partial funding for a new mass storage system was made available from the USGS in mid-year, but the purchase of the new mass storage system had been deferred in an attempt to acquire higher density drives, which ultimately were not available. The new mass system was purchased in late spring 1998, and is comprised of a Sun Ultra 450 computer, a 1.3 Tbyte DISC 517 slot jukebox with two 2.6 GByte Magneto Optical (MO) drives, an 11-slot AIT tape jukebox which holds 25 GBytes per tape, and the SAM-FS hierarchical filesystem management software. Only two MO drives and minimal media were purchased at that time.

This year, the mass storage system was upgraded from its initial 1.3 TByte capacity to 2.5 TByte capacity by the replacement of its 2.6 GByte MO drives by four 5.2 GByte MO drives and 5.2 GB MO media. The mass storage system can be upgraded to a total of 1000 slots (5.2 TByte) capacity with the addition of a second media picker, drives, and media cells.

The older NCEDC data stored on the original two 300 GByte Sony WORM jukeboxes are currently being migrated to the new mass storage system in order to reduce maintenance and operating costs and increase the speed of access to the data. The data migration should be completed by the end of 1999.

The new hardware and software system can be configured to automatically create multiple copies of each data file. The NCEDC is using this feature to create an online copy of each data file on MO media, and another copy on AIT tape which will be stored offline.

4. Joint Northern California Earthquake Catalog

Currently both the USGS and BSL construct and maintain earthquake catalogs for northern and central California. The "official" UC Berkeley earthquake catalog begins in 1910, and the USGS "official" catalog begins in 1966. Both of these catalogs are archived and available through the NCEDC, but the existence of 2 catalogs has caused confusion among both researchers and the public. The BSL and the USGS have spent considerable effort over the past year to define procedures for merging the data from the two catalogs into a single northern and central California earthquake catalog in order to present a unified view of northern California seismicity. The differences in time period, variations in data availability, and mismatches in regions of coverage all complicate the task.

From 1910 through 1967, the BSL catalog is the primary source of northern California earthquake information. Only limited phase data are available for this time period, although location and magnitude information is provided. The NCSN began to come online in 1966, and observations from this network are available beginning in July of that year.

Starting with data from 1996, the BSL and USGS are working to generate a "joint" catalog by merging phase data and relocating the earthquakes. One of the initial complications in this project is matching up events between the two catalogs. Due to the sparse nature of the BSL instrumentation over the years, the BSL catalog is only complete at the magnitude 3 level while the USGS catalog is generally complete at the magnitude 2 level. However, the BSL catalog includes regional events from southern California, Nevada, Utah, Oregon, and Washington. Thus neither catalog is a subset of the other. Other complications include foreshock/aftershock sequences, where one organization might read a foreshock and the mainshock and the other might read the mainshock and an immediate aftershock. Since limited phase data are available for the BDSN until 1976, most events during this period will combine the USGS location with the BSL magnitude. Where BSL phase data are available, an event that appears in both catalogs will have its phase and amplitude data merged, the event will be relocated with the combined phase data, and magnitudes will be recomputed using the available amplitude readings and new location.

The process of consolidating the BSL data to be merged into the joint catalog has uncovered many details in the original catalog which were ambiguous or poorly documented or inconsistent over time, such as the use of channel names for phase and amplitude readings. Significant time has been spent resolving these issues before the joint catalog was actually constructed.

The USGS and BSL performed an initial joint catalog from the USGS and BSL catalogs in the spring of 1999. The BSL spent considerable time analyzing the resulting catalog, and has identified problems with specific earthquake associations and other related problems. We anticipate creating a final merged catalog within the next year.

5. Database Development

Most of the parametric data archived at the NCEDC, such as earthquake catalogs, phase and amplitude readings, waveform inventory, and instrument responses have been stored in flat text files. Flat file are easily stored and viewed, but are not efficiently searched. Over the last year, the NCEDC, in collaboration with the USGS/SCEC Data Center, and TriNet, has continued development of database schemas to store the parametric data from the joint earthquake catalog, station history, complete instrument response for all data channels, and waveform inventory.

The parametric schema supports tables and associations for the joint earthquake catalog. It allows for multiple hypocenters per event, multiple magnitudes per hypocenter, and association of phases and amplitudes with multiple versions of hypocenters and magnitudes respectively. The instrument response schema represents full multi-stage instrument responses (including filter coefficients) for the broadband dataloggers. The hardware tracking schema will represent the interconnection of instruments, amplifiers, filters, and dataloggers over time. This schema will be used to store the joint northern California earthquake catalog and the CNSS composite catalog.

The entire description for the BDSN network and data archive has been entered into the hardware tracking, SEED instrument response, and waveform tables. Programs have been developed to perform queries of waveform inventory and instrument responses, and the NCEDC can now generate full SEED volumes from the BDSN network based on information from the database and the waveforms on the mass storage system. The second stage of development will include the NCSN waveform inventory and later the NCSN instrument response data as they are made available.

Additional details on the joint catalog effort and database schema development may be found at `http://quake.geo.berkeley.edu/db`

6. NETDC

In a collaborative project with the IRIS DMC and other worldwide datacenter, the NCEDC has helped develop and implement NETDC, a protocol which will provide a seamless user interface to multiple datacenters for geophysical network and station inventory, instrument responses, and data retrieval requests. The NETDC system is currently operational in beta test mode between the NCEDC and the IRIS DMC, and was demonstrated at the IUGG meeting in Europe this summer. The NETDC implementation at the NCEDC makes significant use of the waveform and instrument response data stored in our newly developed database. It is scheduled to be opened to public access at the time of the Fall'99 AGU meeting.

Chapter 8

Network Data Analysis

Lind Gee, Doug Neuhauser, Steve Fulton, Rick McKenzie, Asya Kaverina, Doug Dreger, Hrvoje Tkalčić, Bob Uhrhammer

1. Rapid Earthquake Data Integration System

Rapid access to reliable information is critical for any emergency response effort. In the case of a major earthquake, the mobilization of local, state, and federal disaster operations can be greatly enhanced by dependable, near real-time estimates of location, magnitude, mechanism, and extent of strong-ground shaking. This information can be used to identify endangered communities, to evaluate the impact on lifelines, and to provide input for damage and loss estimation programs. Current applications of rapid earthquake information include the emergency services, transportation, utilities, telecommunications, and insurance industries.

Over the last 6 years, the BSL has invested in the development of the hardware and software necessary for a rapid earthquake notification system. The Rapid Earthquake Data Integration (REDI) project is a research program at the BSL for the rapid determination of earthquake parameters with three major objectives: to provide near real-time locations and magnitudes of northern and central California earthquakes; to provide estimates of the rupture characteristics and the distribution of ground shaking following significant earthquakes, and to develop better tools for the rapid assessment of damage and estimation of loss. A long-term goal of the project is the development of a system to warn of imminent ground shaking in the seconds after an earthquake has initiated but before strong motions begin at sites that may be damaged.

1.0.1 Current Status

On April 18, 1996, the BSL and the USGS announced the formation of a joint notification system for northern and central California earthquakes (*Gee et al.,* 1996b). The system merges the programs in Menlo Park and Berkeley into a single earthquake notification system, combining data from the NCSN and the BDSN. On the USGS side, incoming analog data from the NCSN are digitized, picked, and associated as part of the Earthworm system (*Johnson et al.*, 1995). Preliminary locations, based on phase picks from the NCSN, are available within seconds, based on the association of a few arrivals, while final locations and preliminary coda magnitudes are available within 2-4 minutes. Earthworm reports events - both the "quick-look" 25 station hypocenters (without magnitudes) and the more final solutions (with magnitudes) to the Earlybird alarm module in Menlo Park. This system sends the Hypoinverse archive file to the BSL for additional processing, generates pages to USGS and UC Berkeley personnel, and updates the northern California earthquake WWW server.

On the UC Berkeley side, the Hypoinverse archive file is used to drive the REDI processing system. This is a modification of the original REDI design, which identified and located events using raw phase data from the BDSN and NCSN (*Gee et al.,* 1996a). In the revised REDI processing, the magnitude of each hypocenter is assessed. If the coda magnitude is greater than or equal to 3.0, waveforms from the BDSN are analyzed to estimate local magnitude. Once an updated magnitude is obtained, the event information is paged to USGS and UC Berkeley personnel, notification is sent to emergency response agencies, and the revised magnitude is transmitted to the Earlybird system in Menlo Park. The earthquake is then evaluated for the next level of REDI processing. If the local magnitude is greater than 4.5, waveforms from the BDSN strong-motion instruments are analyzed to determine peak ground acceleration, velocity, and displacement and to estimate the duration of strong shaking. When the strong-ground motion processing is complete, these values are distributed by email and pager and the event is scheduled for moment tensor estimation. In this stage of REDI processing, both the waveform modeling method of *Dreger and Romanowicz* (1994) and the surface wave inversion technique of *Romanowicz et al.* (1993) are run for every qualifying event (earthquakes with M_L greater than 3.5). Each algorithm produces an estimate of the seismic moment, the moment tensor solution, the centroid depth, and solution quality. The REDI system uses the individual solution qualities to compute a weighted average of moment magnitude, to compare the mechanisms using normalized root-mean-square of the moment tensor elements (*Pasyanos et al.*, 1996), and to determine a "total" mechanism quality.

In the current implementation, the resulting estimate of moment magnitude is used in preference to local magnitude when the solution quality exceeds 50%. The moment tensor is distributed automatically only when the correlation between the two methodologies exceeds 0.5 and the solution quality is greater than 50%. The moment magnitude information is routinely distributed as part of the REDI system, while the mechanism information is distributed to individuals such as David Hill (in order to assist with the rapid assessment of the Long Valley status) and Jack Boatwright (for his development of methodologies for predicting strong ground shaking) of the USGS and to the OES. Analysts at the BSL review the automatic moment tensor solutions within minutes following an earthquake and distribute updated information.

At present, two Earthworm-Earlybird systems in Menlo Park feed two REDI processing systems at UC Berkeley (Figure 8.1). One of these systems is the production or paging system; the other is set up as a hot backup. The second system is frequently used to test new software developments before migrating them to the production environment. In addition, the BSL operates a third system, which uses BDSN picks to form an independent list of associated events. This third system provides redundancy in case the communication links with the USGS Menlo Park are disrupted. A fourth system, discussed below, is installed in Sacramento (Figure 8.2) in order to provide a redundant notification facility outside of the Bay Area.

This structure has greatly expedited automatic earthquake processing in northern California (Table 8.1). The dense network and Earthworm-Earlybird processing environment of the NCSN provides rapid and accurate earthquake locations, low magnitude detection thresholds, and first-motion mechanisms for smaller quakes. The high dynamic range dataloggers, digital telemetry, and broadband and strong-motion sensors of the BDSN and REDI analysis software provide reliable magnitude determination, moment tensor estimation, peak ground motions, and source rupture characteristics. Robust preliminary hypocenters are available about 25 seconds after the origin time, while preliminary code magnitudes follow within 2-4 minutes. Estimates of local magnitude are generally available 30-120 seconds later, and other parameters, such as the peak ground acceleration and moment magnitude, follow within 1-4 minutes.

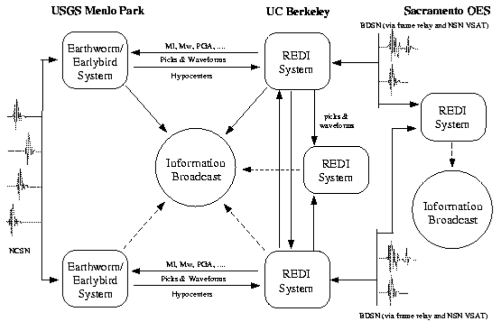

Figure 8.1: Schematic diagram illustrating the connectivity between the real-time processing systems at the USGS Menlo Park and UC Berkeley. The combined system forms the joint earthquake notification project in Northern California. *Courtesy of L. Gee.*

Earthquake information from the joint notification system is distributed by pager, e-mail, and the WWW. The first two mechanisms "push" the information to recipients, while the current Web interface requires interested parties to actively seek the information. Consequently, paging and, to a lesser extent, e-mail are the preferred methods for emergency response notification. The Northern California Web site has enjoyed enormous popularity since its introduction and provides a valuable resource for information whose bandwidth exceeds the limits of wireless systems and for access to information which is useful not only in the seconds immediately after an earthquake, but in the following hours and days as well.

1.0.2 System Performance

The August 12, 1998 earthquake near San Juan Bautista provides a simple example of the joint notification system (*Uhrhammer et al.*, 1998). Although this is

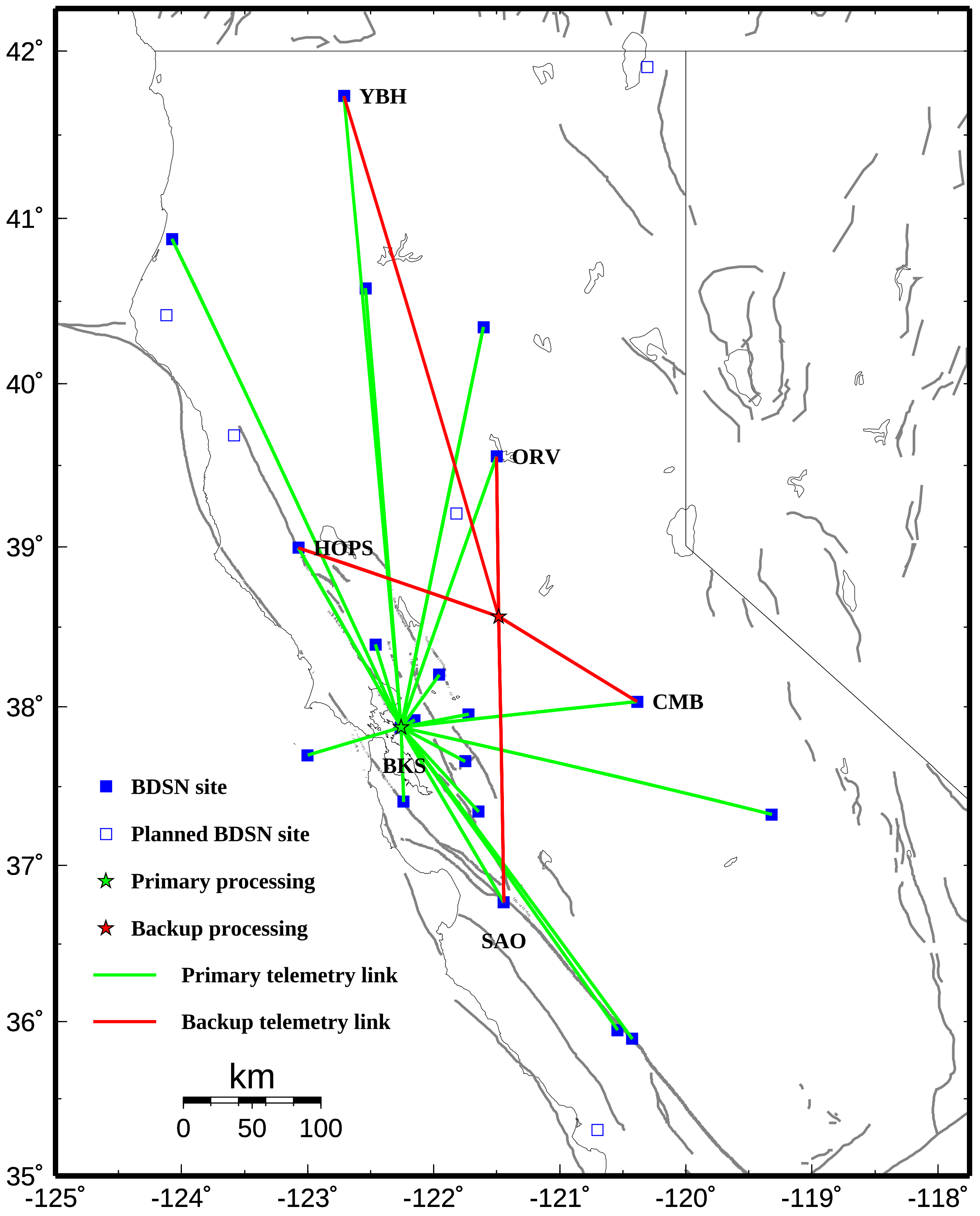

Figure 8.2: Map illustrating the distribution of BDSN stations (squares) used in REDI processing at UC Berkeley and at the redundant processing facility in Sacramento. 6 stations transmit data to both sites. *Courtesy of L. Gee.*

Stage	Qualification	Processing
1	All events	Location
2	M > 3.0	Local magnitude, *Energy magnitude*
3	M > 4.5	Peak ground motion, *Centroid estimation*
4	M > 3.5	Moment tensor
5	M > 6.0	*Line source finite fault*
6	M > 6.0	*2D finite fault*

Table 8.1: Current REDI processing stages. The location procedures in Stage 1 are skipped in normal operation of the joint system, but are utilized if problems prevent the flow of hypocenter information from the USGS. The items in italics are planned extensions to the REDI system.

relatively minor event (5.3 Md, 5.3 Ml, 5.2 Mw; the only reported injuries were a teenager falling from a bunk bed and a painter falling from a ladder (San Francisco Chronicle, 8/13/98)), it is notable as the first event for which the REDI system paged strong-ground motion data.

The first alert of the event at the BSL came when the threshold signal detector at the station BKS triggered (except, of course, for those personnel who felt the earthquake) at 22 seconds after the origin. The BSL monitors the threshold detector at BKS as a preliminary indicator of an event of interest. Triggering at a velocity of 10 microns/sec, the "seismic alarm" notifies BSL personnel by pager and serves as a "wake-up call" (literally, in this case) that an event is in progress. This seismic alarm page is one example of continuous data processing at the BSL.

A "quicklook" location from the Earthworm system, utilizing data from the Northern California Seismic Network at the USGS Menlo Park, was produced within 30 seconds, based on P-wave detections at the nearest 25 stations. A final automatic solution with a coda magnitude of 5.3 was transmitted to the REDI processing system at UC Berkeley 217 seconds at the event occurred and posted on the Web page.

The REDI processing system utilizes data from the Berkeley Digital Seismic Network for the determination of local magnitude, ground motions, and the seismic moment tensor. Using the preliminary magnitude as a guide, the REDI system processed BDSN waveforms from 14 stations to determine a local magnitude of 5.4. The Earthworm location and the REDI local magnitude were paged 272 seconds after the event and the magnitude information was transmitted to the USGS. Data from BDSN strong motion instruments were processed and peak ground accelerations that exceeded 0.5% "g" were distributed by pager (12% g was observed at the BDSN station SAO, which is located 1 km from the epicenter). In the final step of automated processing for this event, the seismic moment tensor and moment magnitude were determined. The automatic moment magnitude of 5.1, the strike-slip mechanism (130/ 89/-164) and the centroid depth of 8 km compare extremely well with the compare extremely well with the reviewed solution of magnitude 5.1, mechanism (129/ 85/-171) and depth of 8 km. All REDI processing was complete a total of 11 minutes after the origin of the event.

Although a small event, this earthquake was widely felt. And the automatic earthquake information produced by the UCB/USGS system provided valuable information to the emergency response managers. For example, the Peninsula Commute Service, which operates train on the San Francisco Peninusla was able to decide that only 1 train of the 14 running from Gilroy to San Francisco needed to be stopped while the track was inspected.

1.0.3 Local and Teleseismic Picker

We are in the final stages of the development of a realtime phase picking algorithm using 3-component broadband waveforms from the BDSN. Recent efforts have focused on improvements to the picker to enhance the performance of the association algorithm. We have encountered two problems in this area. First, the association algorithm can be confused by a multiple P-picks at the same station. In this case, the picker "repicks" immediately following a phase detection. This is a well-known problem and one end-member solution is to reject redetections within some fixed length window following a pick. This approach is typically employed in event detectors, such as the Murdock–Hutt–Halbert algorithm (*Murdock and Hutt*, 1983) installed on the Quanterra dataloggers. We wish, however, to retain sensitivity to the situation where a small event preceeds a larger event and to avoid the problem of "event echos" which can occur when the detection algorithm turns back on. Second, in view of the sparseness of the BDSN, S-wave picks are critical for the location of events outside the network.

In order to address these problems, we have reformulated the characteristic function to include a polarization term (e.g., *Montalbetti and Kanasewich*, 1970). We have also continued to experiment with filters. After some trial and error, we have thrown away the bandpass filter that formed the basis of our previous work. Although the filter enhanced the signal strength, particularly for small events, we have found that the polarization term compensates for this loss with fewer problems from crustal P-waves.

We are currently using a characteristic function of the form:

$$f(t) = av(t)^2 + b(\delta v(t)/\delta t)^2 + c(\delta\theta(t)/\delta t)^2 + d(\lambda(t))^2$$

where $v(t)$ is the velocity, $\theta(t)$ is the change of the solid angle of the velocity vector, $\lambda(t)$ is maximum eigenvalue from the polarization decomposition, and a, b, c, and d are weighting factors. A high-pass filter at 100 sec is applied to the data in order to remove long-period noise from the timeseries before forming the characteristic function.

We are currently running the picker as part of a REDI environment on a test system. The picker is feeding the association algorithm and we are "tuning" the process. The binder algorithm was designed for a dense network such as the NCSN (*Johnson et al.*, 1995) which does not typically observe S phases. Over the last few years, we have gained some experience in using binder with the Murdock-Hutt event detections from the BDSN. However, we are currently experimenting with the balance in weighting S arrivals relative to P and incorporating the "quality" of the arrival. Since the day-to-day seismicity does not, in general, provide us with events of the necessary size for testing, we have developed the capability to feed archive waveform data into the picker.

We have also examined the picker's ability to estimate the azimuth of an incoming arrival based on the use of the polarization filter. We have found that while the picker produces computationally stable estimates of azimuth, comparison with the observed azimuth shows an uncertainty of $+/-20^o$ (Figure 8.4). Although most of the scatter is in the picker estimates, the analyst estimates show considerable variation. We believe that some of the scatter is due to 3-D structure, although a significant component may be introduced by the FIR filters in the Quanterra dataloggers. The FIR filters can also influence the determination of the pick time and we are currently reviewing the possibility of removing the FIR filter in near real-time.

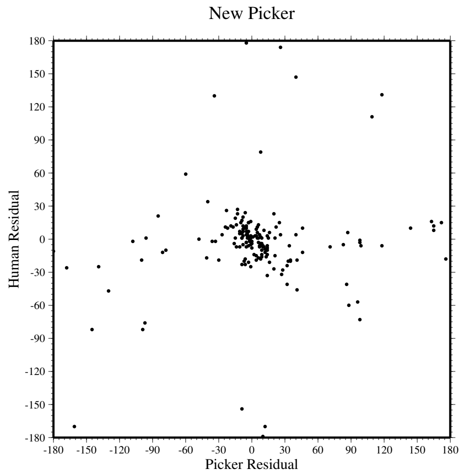

Figure 8.4: Plot of azimuth residual, displaying the scatter from the picker. The "Human Residual" is the difference between the azimuth determined by an analyst and the true source-receiver azimuth while the "Picker Residual" is the difference between the picker estimate and the true source-receiver azimuth. Although most of the scatter is in the picker estimates, the analyst estimates show considerable variation. *Courtesy of S. Fulton.*

1.0.4 Energy Magnitude

One of the important parameters generated by the REDI system is an estimate of earthquake size. The current processing provides estimates of local magnitude, based on Wood-Anderson synthetic amplitudes, and moment magnitude, based on moment tensor procedures. The problem of the saturation of the local magnitude scale is well known and we have relied on moment tensor algorithms to provide a more robust estimate of earthquake size. However, energy magnitude may a better predictor of potential damage than moment magnitude, since the energy represents the integral of the spectrum over the entire frequency band. Consequently, we are preparing to expand the capabilities of the REDI system to include energy magnitude.

We have calibrated the algorithm of *Kanamori et al.* (1993) for northern California. Using a suite of 152 earthquakes, we have determined estimates of seismic energy release using:

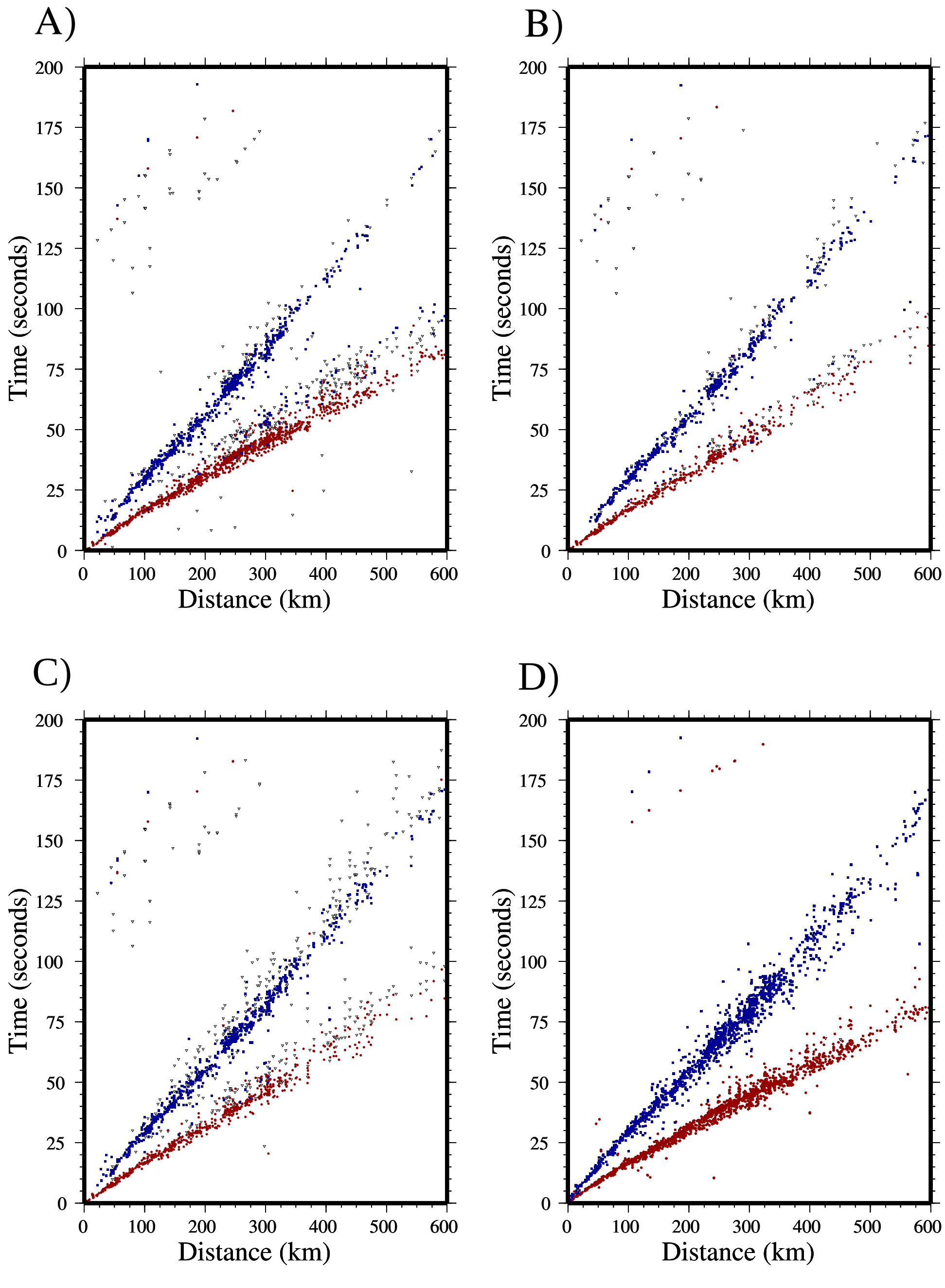

Figure 8.3: Figure comparing the results of different versions of the picker algorithm, plotted as travel time versus distance, for 128 earthquakes, and the UC Berkeley analyst's picks for the same events. A) The original characteristic function combined with a bandpass filter. B) The original characteristic function without the bandpass filter. Notice the the decrease in the number of P and S picks, as well as the decrease in the "post-P" detections. C) The new characteristic function without the bandpass filter. D) UC Berkeley analyst's picks for this data set. *Courtesy of S. Fulton.*

Station	s_i	No. of obs	M_L adjustment
ARC	0.2808	126	+0.209
BDM	0.5177	49	-0.023 *
BKS	1.0000	127	-0.035
BRIB	0.7515	89	+0.176
BRK	1.6369	97	+0.198
CMB	2.8105	127	+0.240
CVS	1.0835	78	-0.189 *
FARB	1.9465	92	-0.150
HOPS	1.1581	114	+0.324
JRSC	0.8514	124	+0.139
KCC	3.6114	96	+0.369
MHC	0.8681	126	+0.128
MIN	0.5680	121	-0.107
ORV	3.7033	127	+0.428
PKD	0.6153	96	-0.033 *
PKD1	0.1420	27	-0.198
POTR	0.2266	41	+0.159 *
SAO	1.3975	125	+0.314
STAN	0.1668	3	-0.233
WDC	2.5639	126	+0.484
WENL	0.4048	82	+0.089 *
YBH	2.1010	126	+0.499

Table 8.2: Station corrections for determination of energy release. For comparison, the M_L station adjustments are included in the table (*Uhrhammer et al.*, 1996). * indicates a preliminary estimate of the adjustment.

$e_{ij} = 23.6x10^5 r^2 [r_o q(r_o)/rq(r)]^2 \int \sum v_{ij}(t)^2 dt$

where e_{ij} is the energy of earthquake j at station i, r is the hypocentral distance, r_o is 8 km, $q(r)$ is the attenuation curve for distance r, v_{ij} is the observed velocity, and the expression includes correction terms for the radiation pattern. We found that the revised attenuation relation of *Kanamori et al.* (1993) provides a good fit to the northern California data and that no addition distance correction are required (Figure 8.5) . On the other hand, significant station variations are observed. In order to reduce the influence of site effects, we fixed the energy estimate at a single station (BKS) and determined site-specific scale factors for the network: $E_j = e_{ij} s_i$ where E_j is the correct estimate of the seismic energy release by earthquake j and s_i is the correction factor for station i.

The correction factors range from 0.14 to 3.7 and correlate, in general, with the local magnitude station corrections (Table 8.2). This is a larger variation in these corrections than observed by southern California, which may reflect the greater variability of geologic conditions at BDSN sites. The coastal stations tend to have similar corrections to BKS, but the stations in the Sierra stand out with their large corrections (CMB, KCC, ORV, WDC, YBH). Figure 8.5 compares the individual estimates of energy as a function of distance with and without the station corrections. The station corrections have significantly reduced the scatter in the energy estimates, although some site effects remain.

Using southern California events, *Kanamori et al.* (1993) obtained a linear relationship between the $\log E$ and local magnitude ($M_E = 0.51(\log E - 9.05)$). We have found that this describes the northern California events well and we plan to implement energy magnitude estimation to the current stage for local magnitude. Under this revised processing, both M_L and M_E would be calculated for every qualified event (earthquakes with coda magnitude greater than 3.0).

1.0.5 Finite Rupture Parameters

Much of the current REDI processing is based on the use of the high-frequency hypocenter location. While this is adequate for most events, a finite rupture becomes increasely important for earthquakes of interest - particular from the perspective of emergency response. We are in the process of expanding the REDI system to include procedures for the estimation of the rupture centroid as well as the determination of finite-fault parameters.

Rupture Centroid The hypocenter location estimated using high-frequency travel times generally represents the point of rupture initiation. For a finite rupture, the centroid of the faulting can provide more useful information for rapid response. One approach to this problem is to estimate the centroid location as part of the moment tensor procedures. However, in the short term, we are exploring the use of amplitude data to estimate a "strong-motion centroid" (*Kanamori*, 1993). This method uses the decay of amplitude with distance in order to determine the most probable event location.

We have tested the procedure on a number of magnitude 5+ events with three types of amplitude data: peak ground acceleration (PGA), peak ground velocity (PGV), and Wood-Anderson synthetic amplitude (WAS). We have experienced some difficulty in using PGA and PGV with the attenuation relations of *Joyner and Boore* (1981), suggesting that these relationships do not hold for moderate earthquakes in northern California (Figure 8.6), especially at distances greater than 100 km. We have had more success using the WAS for this procedure, based on the attenuation relation of *Bakun and Joyner* (1984). This is perhaps not surprising, since

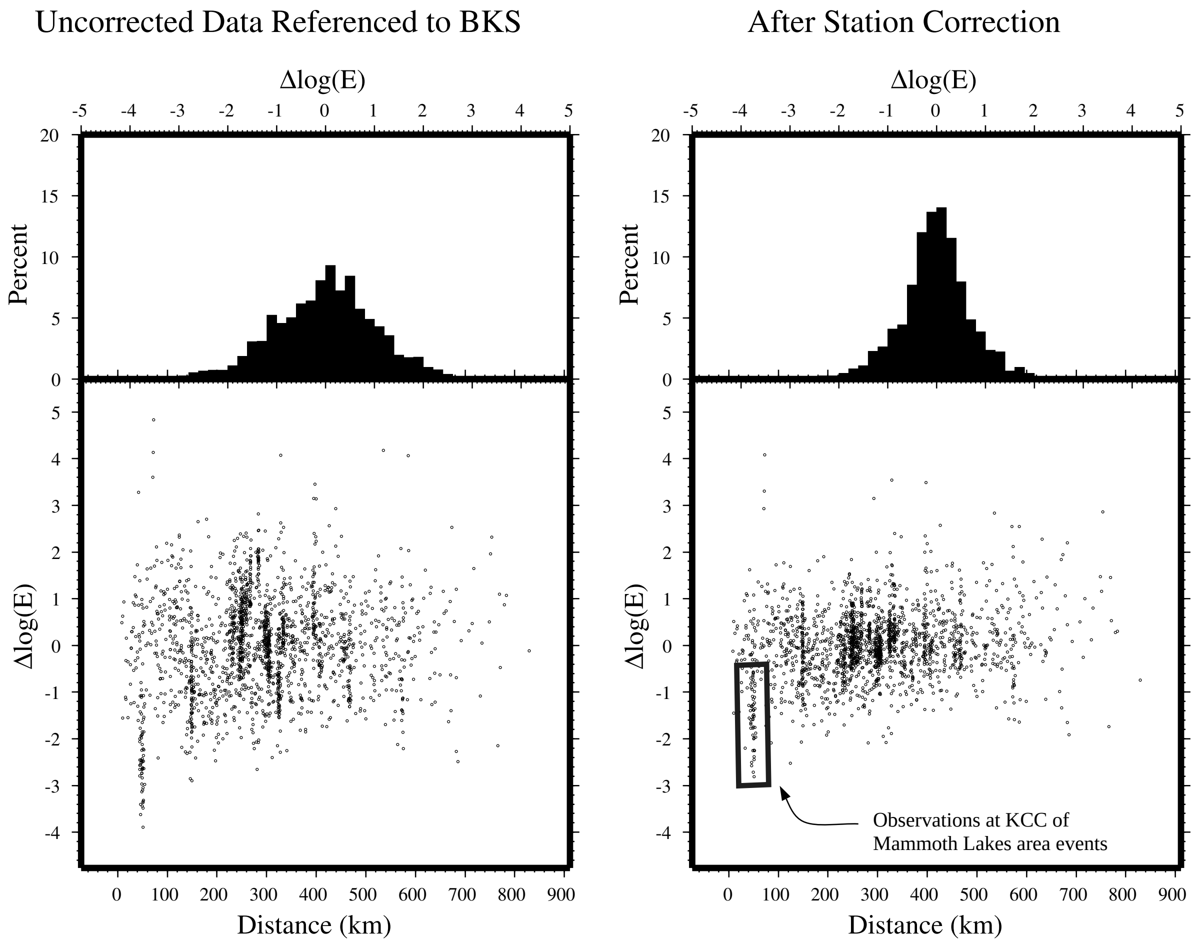

Figure 8.5: Figure illustrating the deviation of $\log E$ as a function of distance, before (left) and after (right) the determination of station corrections. *Courtesy of S. Fulton.*

Case	Latitude	Longitude	Dist (km)
Epicenter	36.7527	-121.4627	4
PGA	36.80	-121.53	10
PGV	36.80	-121.50	10
WAS	36.80	-121.53	10
PGA	36.05	-122.70	67
PGV	36.75	-121.75	67
WAS	36.80	-121.70	67

Table 8.3: Centroid locations obtained from peak ground acceleration (PGA), peak ground velocity (PGV), and Wood-Anderson amplitudes (WAS) from BDSN stations. For each amplitude type, the centroid is estimated with and without the nearest station, SAO. The centroid estimate is strongly dependent on the station distribution.

we use the Wood-Anderson amplitudes to estimate local magnitude, but we use the Nordquist nomograph rather than this analytic relationship. The TriNet project is also using Wood-Anderson amplitudes to determine the strong-motion centroid (*Wald et al.*, 1999).

We have found that this procedure is strongly dependent on the distribution of stations. The case of the 8/12/1998 M5.3 earthquake in San Juan Bautista illustrates this effect (Figure 8.7). The centroid estimation procedure works well for the San Juan Bautista earthquake (since the nearest BDSN station is within a few kilometers). However, if the data from the closest station is removed, then a significant degradation is observed (Table 8.3). In this example, the PGA estimate of the centroid is within 2 km of the high-frequency location, while the PGV and WAS estimates are closer to the end of the aftershock zone, approximately 8 km to the northwest. When the closest station is removed, however, all three estimates move west, with the PGA estimate moving over 135 km.

Similar behavior has been observed in other recent events, such as the 08/18/1999 Bolinas earthquake where the nearest BDSN station was over 35 km away and the distribution of stations was rather one-sided. As a result, a poor estimate of the centroid is obtained.

We are currently adding the centroid estimation procedure to the existing REDI stage of strong-ground motion processing. However, the results of this alogrithm need to be treated judiciously, depending on the distribution of stations. As the density of digital instrumentation increases in the San Francisco Bay Area, this sensitivity will be reduced. However, this is likely to remain a problem in less populated areas where the density of instrumentation may not significantly increase.

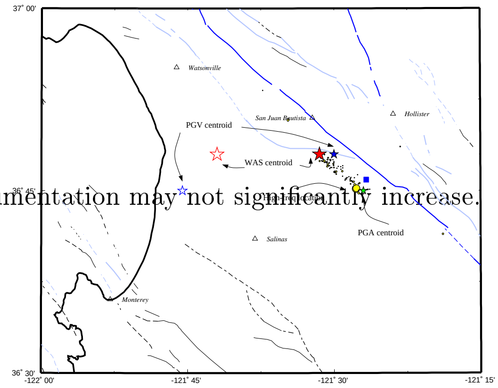

Figure 8.7: Map displaying different centroid locations for the San Juan Bautista earthquake (circle) determined from WAS, PGA, and PGV. The filled stars are solutions obtained using data from SAO (square) while the open stars are solutions with data from SAO. Note that the PGA solution without SAO does not locate on the map. *Courtesy of L. Gee.*

Finite Fault Parameterization We have made progress toward the goal of expanding REDI processing to include the estimation of finite-fault parameters. When completed, this development will add two new stages to the REDI processing structure with the goal of automatically estimating the distribution of slip on a finite-fault plane from regional-distance seismograms.

As the first step in this development, we are automating the existing codes (*Dreger and Kaverina*, 1999 - described in detail in the research section). Programs developed for interactive use in a research environment require significant effort to structure and harden for an operational environment and our recent efforts have focused in this direction. We have divided the finite-fault estimation procedure into 2 REDI stages. In the first stage, BDSN regional waveform data are prepared for inversion and preliminary or initial estimates of the rupture parameters are derived using empirical scaling relationships.

These empirical estimates are then checked by testing a line-source rupture either along the rake or in the horizontal plane. Studies of the Landers and Northridge earthquakes (*Dreger and Kaverina*, 1999) suggest that the horizontal line source may work better. The line source calculation can be computed quite rapidly and it is possible to test a range of rupture velocities as well as both possible fault planes in order to identify the causative fault.

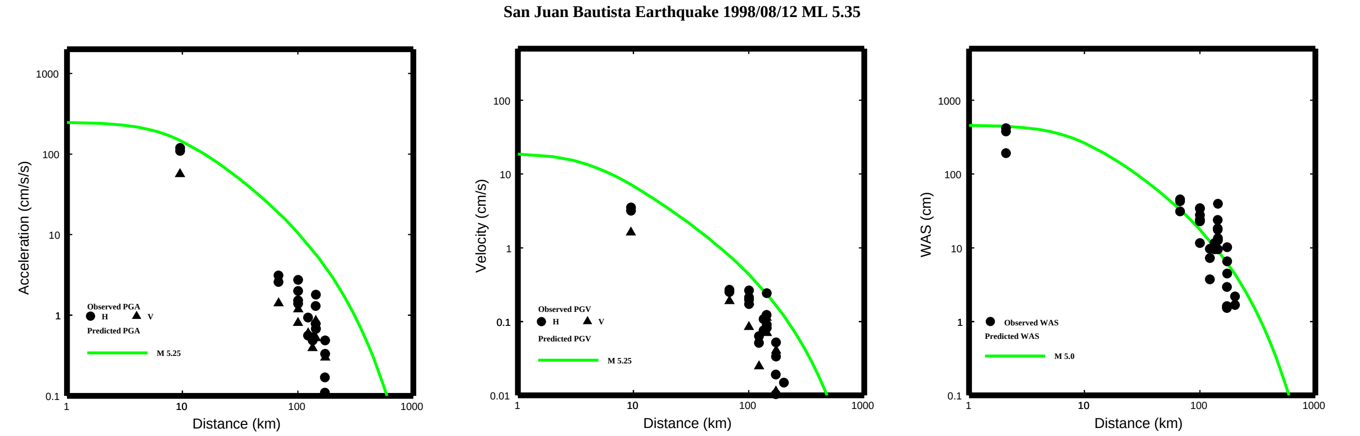

Figure 8.6: Figure illustrating the fit of BDSN observations to attenuation relationships for peak ground acceleration, peak ground velocity, and Wood-Anderson amplitudes for the M5.3 San Juan Bautista earthquake. *Courtesy of L. Gee.*

When completed, this REDI stage will yield preliminary estimates of the rupture length, width, rupture velocity, dislocation rise time, and probable fault plane. These values then become input to the next stage for refinement. Stage 5 will perform the full 2-dimensional inversion for distributed slip on both fault planes and will produce a slip map for the preferred plane.

The automation of these codes is nearly complete and we anticipate having them fully incorporated within the REDI structure before the end of 1999. These stages will be executed for earthquakes of moment magnitude 6.0 and higher.

In parallel with this development, we are also working toward the parameterization of fault rupture using GPS. As planned, this system would parallel the REDI processing and provide an independent estimate of the source parameters.

1.0.6 "Shake Maps"

The quantification of a finite rupture is important for emergency response as it may be used to identify communities directly affected by the faulting process. However, these parameters may be used to predict areas of strong shaking following a major earthquake. These "Shake Maps" are highly valued by emergency response personnel (*Wald et al.*, 1999) and have become a routine operation in southern California as part of the TriNet Project.

In northern California, we are working with the USGS and the CDMG to implement capabilities similar to those in southern California. The USGS has taken the lead role in adapting the southern California software to northern California (in particular, correcting for site effects and attenuation relations). At the moment, we are working to development mechanisms to import data from the REDI stage of strong-motion processing to the USGS for map generation.

In the longer term, we plan to implement the generation of shake maps as part of the REDI system. In particular, we intend to both implement the current "approved" procedures (Shake Map Ver 1.0) as well as new methods that take the finite-fault parameters estimated by the REDI system and use the theoretical Green's functions to generate synthetic seismograms for a grid of points. Maps of predicted peak ground acceleration, peak ground velocity, and spectral acceleration will be generated.

1.0.7 Redundant Processing

In a further step to insure that information is available following a major Bay Area earthquake, we have established a backup processing facility in the Sacramento headquarters of the California Office of Emergency Ser-